



HAL
open science

A combined crystallographic analysis and ab initio calculations to interpret the reactivity of functionalized hexavanadates and their inhibitor potency toward $\text{Na}^+/\text{K}^+-\text{ATPase}$

Xiao M Xu, Nada B Bošnjaković-Pavlović, Mirjana M Čolović, Danijela M Krstić, Vesna M Vasić, Jean-Michel Gillet, Pingfan M Wu, Yongge B Wei, Anne M Spasojević-de Biré

► **To cite this version:**

Xiao M Xu, Nada B Bošnjaković-Pavlović, Mirjana M Čolović, Danijela M Krstić, Vesna M Vasić, et al.. A combined crystallographic analysis and ab initio calculations to interpret the reactivity of functionalized hexavanadates and their inhibitor potency toward $\text{Na}^+/\text{K}^+-\text{ATPase}$. *Journal of Inorganic Biochemistry*, 2016, 161, pp.27 - 36. 10.1016/j.jinorgbio.2016.04.029 . hal-01385048

HAL Id: hal-01385048

<https://hal.science/hal-01385048>

Submitted on 24 Sep 2020

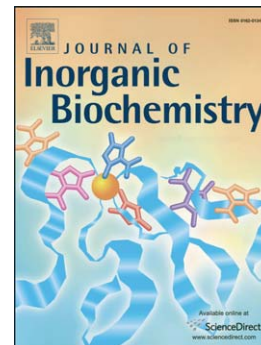
HAL is a multi-disciplinary open access archive for the deposit and dissemination of scientific research documents, whether they are published or not. The documents may come from teaching and research institutions in France or abroad, or from public or private research centers.

L'archive ouverte pluridisciplinaire **HAL**, est destinée au dépôt et à la diffusion de documents scientifiques de niveau recherche, publiés ou non, émanant des établissements d'enseignement et de recherche français ou étrangers, des laboratoires publics ou privés.

Accepted Manuscript

A combined crystallographic analysis and *ab initio* calculations to interpret the reactivity of functionalized hexavanadates and their inhibitor potency toward Na⁺/K⁺-ATPase

Xiao Xu, Nada Bošnjaković-Pavlović, Mirjana B. Čolović, Danijela Z. Krstić, Vesna M. Vasić, Jean-Michel Gillet, Pingfan Wu, Yongge Wei, Anne Spasojević-de Biré



PII: S0162-0134(16)30114-3
DOI: doi: [10.1016/j.jinorgbio.2016.04.029](https://doi.org/10.1016/j.jinorgbio.2016.04.029)
Reference: JIB 9987

To appear in: *Journal of Inorganic Biochemistry*

Received date: 22 November 2015
Revised date: 16 April 2016
Accepted date: 25 April 2016

Please cite this article as: Xiao Xu, Nada Bošnjaković-Pavlović, Mirjana B. Čolović, Danijela Z. Krstić, Vesna M. Vasić, Jean-Michel Gillet, Pingfan Wu, Yongge Wei, Anne Spasojević-de Biré, A combined crystallographic analysis and *ab initio* calculations to interpret the reactivity of functionalized hexavanadates and their inhibitor potency toward Na⁺/K⁺-ATPase, *Journal of Inorganic Biochemistry* (2016), doi: [10.1016/j.jinorgbio.2016.04.029](https://doi.org/10.1016/j.jinorgbio.2016.04.029)

This is a PDF file of an unedited manuscript that has been accepted for publication. As a service to our customers we are providing this early version of the manuscript. The manuscript will undergo copyediting, typesetting, and review of the resulting proof before it is published in its final form. Please note that during the production process errors may be discovered which could affect the content, and all legal disclaimers that apply to the journal pertain.

A combined crystallographic analysis and *ab initio* calculations to interpret the reactivity of functionalized hexavanadates and their inhibitor potency toward Na⁺/K⁺-ATPase

Xiao Xu^{† a, b}, Nada Bošnjaković-Pavlović^{† c}, Mirjana B. Čolović^d, Danijela Z. Krstić*^e, Vesna M. Vasić^d, Jean-Michel Gillet^{a, b}, Pingfan Wu^f, Yongge Wei^g, and Anne Spasojević-de Biré*^{a, b}

^a Université Paris Saclay, CentraleSupélec, Campus de Châtenay, Grande Voie des Vignes, 92295 Châtenay-Malabry, France

^b CNRS, UMR 8580, Laboratory “Structures Propriétés et Modélisation des Solides” (SPMS), Grande Voie des Vignes, 92295 Châtenay-Malabry, France

^c Faculty of Physical Chemistry, University of Belgrade, P.O. Box 47, 11001 Belgrade, Serbia

^d Department of Physical Chemistry, Vinča Institute of Nuclear science, University of Belgrade, P.O.Box 522, Belgrade, Serbia

^e University School of Medicine, Institute of Medical chemistry, University of Belgrade, Višegradska 26, 11000 Belgrade, Serbia

^f Institute of POM-based Materials, The Synergistic Innovation Center of Catalysis Materials of Hubei Province, Hubei University of Technology, 430086 Wuhan, Hubei Province, P. R. China

^g Department of Chemistry, Tsinghua University, 100084 Beijing, P. R. China

[†] XX and NBP have contributed equally

* authors to whom correspondence should be addressed

ABSTRACT

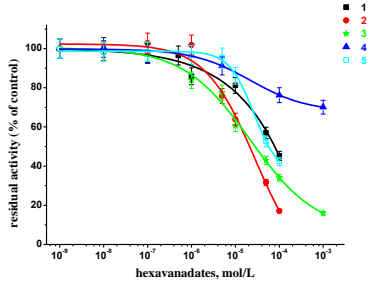
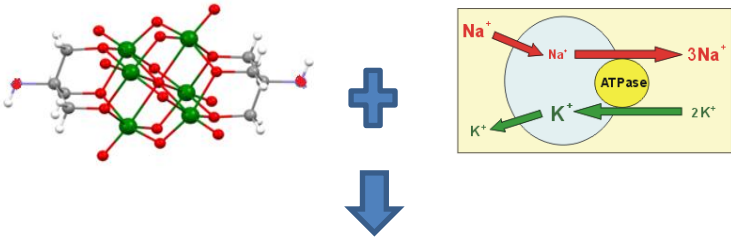
In vitro influence of five synthesized functionalized hexavanadates (V_6) on commercial porcine cerebral cortex Na^+/K^+ -ATPase activity has been studied. Dose dependent Na^+/K^+ -ATPase inhibition was obtained for all investigated compounds. Calculated half maximal inhibitory concentration IC_{50} values, in mol/L, for Na^+/K^+ -ATPase were 7.6×10^{-5} , 1.8×10^{-5} , 2.9×10^{-5} , 5.5×10^{-5} for functionalized hexavanadates (V_6) with tetrabutylammonium (TBA) [V_6-CH_3][TBA]₂, [V_6-NO_2][TBA]₂, [V_6-OH][TBA]₂ and [V_6-C_3][TBA]₂ respectively. [V_6-OH][Na]₂ inhibited Na^+/K^+ -ATPase activity up to 30% at maximal investigated concentration 1×10^{-3} mol/L. This reactivity has been interpreted using a study of the non-covalent interactions of functionalized hexavanadate hybrids through Cambridge Structural Database (CSD) analysis. Bibliographic searching has led to 18 different structures and 99 contacts. We have observed that C-H...O contacts consolidate the structures. We have also performed density functional theory (DFT) calculations and have determined electrostatic potential values at the molecular surface on a series of functionalized V_6 . These results enlightened their chemical reactivity and their potential biological applications such as the inhibition of the ATPase.

Keywords: Functionalized hexavanadate, Na^+/K^+ -ATPase, inhibition, Cambridge Structural Database, non-covalent interactions

Short synopsis

Five compounds of hexavanadates (V_6) were synthesized and their inhibitor potency toward Na^+/K^+ -ATPase was investigated. Investigated hexavanadates showed inhibitory effect on Na^+/K^+ -ATPase activity. Analysis of noncovalent interactions between V_6 and organic part using the Cambridge Structural Database was performed.

Graphical abstract



1. Introduction

Polyoxovanadates (POVs) are one of the most important series in the large family of polyoxometalate (POMs), due to their wide structure diversity. POVs are a very interesting kind of vanadium-containing compounds due to the fascinating electronic and magnetic properties, various thermodynamically stable redox isomers, and catalytic capabilities [1, 2]. In 1983, M. T. Pope illustrated, that vanadium, in its higher oxidation state, gives many isopolyvanadates ranging from metavanadates chains $[\text{VO}^{3-}]_n$, to layered oxides $[\text{V}_2\text{O}_5]$ and compact polyanions $[\text{V}_{10}\text{O}_{28}]^{6-}$ [1]. Even polyanionic hollow cages such as $[\text{V}_{15}\text{O}_{36}]^{5-}$, in which anions are encapsulated, have been reported [2]. Such a rich structural chemistry is due to the ability of vanadium to adopt a variety of coordination geometries, $[\text{VO}_6]$, $[\text{VO}_5]$, $[\text{VO}_4]$ units and different oxidation states (V^{V} , V^{IV}). Hexavanadates (V_6), one of an important series of POVs, exists as inorganic-organic hybrids (Figure 1). After the initial characterization of $[(\text{C}_5\text{Me}_5)\text{Rh}]_4(\text{V}_6\text{O}_{19})$ by Chae [3] and Hayashi [4,5], a large number of new polyoxovanadates and their related properties were mainly reported by several groups of Müller, Zubieta [8-10], Hill [11,12], Hayashi [13], T. B. Liu [14], Wei [15,16], and Daniel [17] over the last 30 years. Hayashi has described the different species of POV structures such like tetravanadate (V_4 unit), hexavanadates (V_6 unit), decavanadate (V_{10} unit), dodecavanadate (V_{12} unit), and other heteropolyoxovanadates, lacunary POV, providing a better understanding on the classification of POVs complicated structures [13].

Recently, we found that POVs exhibit potential bioactivities, especially the inhibition of Na^+/K^+ -ATPase [18]. Dose-dependent inhibition of plasma membrane Ca^{2+} -ATPase (PMCA) and sodium pump by V_{10} as well as kinetic analysis, is in agreement with previously reported findings that V_{10} species block the active side of P-type ATPases. Consequently, it affects phosphorylation step in the enzyme cycle of P-type ATPases (sodium and calcium pump) [19]. Na^+/K^+ -ATPase (sodium pump) belongs to the P-type ATPase family, which are able to utilize the energy of ATP to transport ions against their electrochemical gradient. Na^+/K^+ -ATPase is a cell membrane located in enzyme and maintaining the high internal K^+ and low internal Na^+ concentrations, characteristic and essential for normal cellular activities of most animal cells [20,21]. The activity of this enzyme is very sensitive to the presence of some metal ions and organic compounds of various structures, especially in the case of some drugs and pesticides [22]. Na^+/K^+ -ATPase has been chosen due to its key role in normal functioning of most cells of higher eukaryotic organisms [23,24] and in development and progression of different cancers [25], as well as the known influence of POMs on nucleotide-

dependent enzymes [26-28] and their anti-cancer and anti-viral activity. Investigation of the POMs interactions with peptides or proteins, which play a fundamental role in biological systems, has been a subject of growing interest in recent years [29]. It was reported that V_{10} is the major protein-bound species of vanadium and has a stronger inhibitory effect on various enzymes, when compared to other vanadate oligomers [30]. V_{10} studies include also the possibility of its use as a tool in the understanding of the transducing chemical energy into conformational energy for Ca^{2+} transport by Ca^{2+} -ATPase [31] as well as molecular mechanism of muscle contraction [32]. Inhibitions of several ATPases such as P-type ATPases, ABC-ATPases and ribonucleases by V_{10} suggest that V_{10} interactions with these proteins are probably favored by the existence of an ATP binding site [28]. More recently the exceptional biological activity of V_{10} has been reviewed by Aureliano [33]. These studies illustrate the importance of the noncovalent interactions between vanadate species and peptides. It is clear that vanadate interacts strongly with positively charged proteins. At a molecular level, the mechanism of action is played *via* noncovalent interactions between the V_{10} anion and the biological target [34,35]. This information could be useful for understanding the potential reactivity of V_6 hybrids (Figure 1). Additionally, V_{18} presents antitumor activity inhibiting the growth and proliferation of human cancer cells and has a low toxicity on human normal cells *in vitro* [36]. The mechanism for the antitumor effect of polyoxomolybdate has been established; it concerns a single electron reduction oxidation cycle in isopolymolybdates [37-39]. According to this hypothesis, the inhibitory activity of POMs on tumor cells is relevant to the oxidation reduction ability: the stronger the oxidation capability, the higher the inhibitory effect on tumor cells.

From a geometric point of view, the $[V_6O_{19}]^{2-}$ (simplified as V_6) anion is represented in Figure 1a. According to their vanadium coordination, the oxygen atoms could be classified as follows. Four types of oxygen atoms are involved in this anion: O1x - bonded to only one vanadium atom; O2x - shared between two vanadium atoms; O3x - connected with two vanadium atoms and organic ligand; O6x - have a six-fold coordination of vanadium atoms. Oxygen atoms of a V_6 anion are attractive sites, and therefore can form intermolecular hydrogen bonds. Many weak hydrogen bonds are found between V_6 anions and organic segments. The statistical analysis of these non-covalent interactions between V_6 anion and organic segments using the Cambridge Structural Data Base (CSD) can provide structural evidence for the biological role of the V_6 anion. Crystal structures of the title compounds are stabilized by an extensive C-H...O hydrogen bonding network, which involves the V_6 anions

and organic segments. Hydrogen bonds and their environment have a well-defined geometry in the crystalline state. CSD provides a large amount of experimental data that allows hydrogen bonds geometries to be analyzed with good statistics [41]. Therefore, CSD is a major source of knowledge on intermolecular interactions of all types. A major contribution of CSD analysis has been the identification of weak hydrogen bonds such as $\text{CH}\cdots\text{O}$ or $\text{CH}\cdots\pi$ [42-44].

In this study, we have synthesized five V_6 to investigate the *in vitro* effect of V_6 on commercial porcine cerebral cortex Na^+/K^+ -ATPase activity. In order to understand the obtained results, we have retrieved the V_6 based compound structures from the CSD, and determined the intermolecular interactions between V_6 oxygen atoms and the proton donor. We have also determined theoretical electrostatic potential (EP) from *ab initio* calculations.

2. Material and methods

2.1. Synthesis of V_6 compounds

Preparation of $[\text{V}_6\text{-CH}_3][\text{TBA}]_2$ (TBA tetrabutylammonium) (compound **1**). **1** has been synthesized according to the route described by Chen et al [8]. Preparation of $[\text{V}_6\text{-NO}_2][\text{TBA}]_2$ (compound **2**). **2** has been synthesized according to the route described by Chen *et al* [48f]. Preparation of $[\text{V}_6\text{-OH}][\text{TBA}]_2$ (compound **3**). **3** has been synthesized according to the route described by Wu *et al* [45]. Preparation of $[\text{V}_6\text{-OH}][\text{Na}]_2$ (compound **4**). **4** has been synthesized according to the route described by Wu *et al* [45]. Preparation of $[\text{V}_6\text{-C}_3][\text{TBA}]_2$ (compound **5**). **5** has been obtained according to the route described by Wu *et al* [46].

2.2. Preparation of V_6 solutions

Stock solutions (0.1 mol/L) of **1**, **2**, **3** and **5** were prepared by solving the solid compounds in DMSO, while **4** stock solutions was prepared in aqueous solution. Working solutions were prepared daily by water dilution of the stock solutions to the desired concentrations, shortly before use.

2.3. Na^+/K^+ -ATPase assay

The standard assay medium for investigation of Na^+/K^+ -ATPase activity contains (in mmol/L): 50 Tris-HCl (pH 7.4), 100 NaCl, 20 KCl, 5 MgCl_2 , 2 ATP and 290 mg/L

commercially available porcine cerebral cortex proteins in a final volume of 200 μL . After pre-incubation for 10 min at 37°C and control of the appropriate concentration of the investigated V_6 compounds, the reaction was initiated by addition of ATP and stopped after 20 mins by adding 22 μl of 3 mol/l ice cold HClO_4 and immediate cooling on ice. Final DMSO volume fraction in the incubation medium does not exceed 1%. The released inorganic phosphate group (P_i) liberated from the hydrolysis of ATP was determined by a modified spectrophotometric method [47]. Spectrophotometric measurements were performed on a Perkin Elmer Lambda 35 UV VIS spectrophotometer. Results are expressed as mean percentage enzyme activity compared to the corresponding control value \pm S.E.M. (standard error of mean) of two independent experiments done in triplicate.

2.4. CSD analysis

We have investigated the interactions depending on the oxygen types of V_6 , O1x and O2x , which are on the surface of the molecules. We have focused on the arm-like functionalized V_6 anion with two symmetrical tripodal ligands, which are listed in Table 1. Different structures have been found to contain V_6 anion, leading to 99 intermolecular contacts, which are shorter than the sum of van der Waals radii. In order to avoid crystal structure low quality, the R factor was required to be less than 10. These interactions belong to the 18 structures for which the hydrogen bonds have been localized [48]. For each interaction, depending on the oxygen type O1x and O2x , we have calculated the C-H...O distance and angle. Moreover, we have retrieved protonated V_6 (Table 1) and V_6 based compounds where more than six external oxygen atoms are bridged with organic ligands [49], in order to analyze the reactivity of external oxygen atoms (Table 2).

2.5. Computational details

DFT calculations were performed with Gaussian 09 (EM64L-G09RevC.01) [Frisch, 2010]. Hybrid functionals, which include a mixture of Hartree-Fock exchange with DFT exchange-correlation have been employed (B3LYP: [Becke, 1993]; M06/M06-2X, [Zhao, 2008]. Atomic coordinates of $[\text{V}_{10}\text{O}_{28}]^{6-}$ [34], $[\text{V}_6\text{OH}]^{2-}$ (compound **3** and **4**) [53], and $[\text{V}_6\text{-C}_3]^{2-}$ (compound **1** and **5**) [53] are obtained from the corresponding high resolution X-ray diffraction experimental nuclei positions. Geometric optimization was carried out. Atomic coordinates of compound **2** have been obtained from CSD; the geometry has been optimized

by M06/6-31+G(d, p) quantum chemistry model. The computed densities have converged with cc-pVTZ basic set.

3. Results and discussion

3.1. *In vitro* influence of V₆ compounds on Na⁺/K⁺-ATPase activity

The influence of the five synthesized V₆ compounds (Table 3) on commercial porcine cerebral cortex Na⁺/K⁺-ATPase activity has been investigated by *in vitro* exposure to the enzyme in the concentration range from 1×10^{-9} to 1×10^{-3} mol/L. The results show, in all cases, that increasing concentrations of the investigated compounds induce inhibition of enzymatic activity in a concentration-dependent manner (Figure 2). The experimental dependence of the enzyme activity, expressed as a percentage of the control value (obtained without inhibitor), on inhibitor concentration fits a sigmoidal function (Figure 2).

The inhibition parameters (IC₅₀ values), defined as the concentration of investigated compound with capability to inhibit 50% of the enzyme after given exposure time, were determined using the sigmoidal fit and summarized in Table 3. The obtained results demonstrate that the inhibitory effect on Na⁺/K⁺-ATPase activity was rated as compounds **2** > **3** > **5** > **1** > **4**. Actually, the most potent inhibitor is compound **2** (IC₅₀ = $(1.8 \pm 0.5) \times 10^{-5}$ mol/L), while the compounds **3**, **5** and **1** are several times weaker inhibitors of Na⁺/K⁺-ATPase, which induced half of maximal enzyme activity (control) at concentrations (in mol/L) of $(2.9 \pm 0.3) \times 10^{-5}$, $(5.5 \pm 0.3) \times 10^{-5}$, $(7.6 \pm 0.5) \times 10^{-5}$, respectively. The enzyme is significantly less sensitive toward **4**, i.e. half of maximum enzyme inhibition was not reached at the highest investigated concentration, 1×10^{-3} mol/L.

The obtained results (Figure 2 and Table 3) are in agreement with previously reported concentration-dependent inhibitory effect of polyoxovanadates on synaptic plasma membrane and purified porcine cerebral cortex Na⁺/K⁺-ATPase [18] as well as several nucleotide-dependent enzymes [26,27]. However, V₁₀ has been observed around ten times more potent inhibitor of the purified enzyme [18] compared with investigated V₆ (**1**, **2**, **3** and **5**).

The key factors, which could explain the interaction between V₆ and V₁₀ compounds and Na⁺/K⁺-ATPase are: i) the size of the inhibitor (consistent with the enzyme pocket); ii) the EP express by the inhibitor (in complementary with the EP express by enzyme pocket); iii) the possibility of the inhibitor to build hydrogen bonds or non-covalent interactions with amino acids of the enzyme. In this case, the inhibitor is the functionalized V₆ anion, the

counter ion (TBA or Na^+) is necessary to stabilize the V_6 , but in solution the functionalized V_6 anion is supposed to be isolated. The observed differences between compounds **3** and **4** could be assigned to an additional effect due to the cation. The size of the V_6 series could be modeled by the longest distance between two opposite atoms of the organic arm of the functionalized V_6 compound. Correlation between the size of the compound and the inhibition activity could not be established.

EP values at the molecular surface of the functionalized V_6 series have been determined and plotted (Figure 3). EP can be used as a tool for predicting chemical reactivity, especially for non-covalent interactions. EP values are the most negative in the vicinity of the three oxygen atoms defining the yellow triangle (Figure 3, left column). This provides a predictable pattern for non-covalent interactions and points out the probable chemical reactivity sites. In this type of functionalized V_6 compounds, under a proper condition, O1x and O2x could act as potential reaction sites [54, 55, 49f]. In order to graphically exhibit the intermolecular charge transfer in a better way, between V_6 core and the organic ligand, electrostatic potentials are mapped as isovalue surfaces at $\pm 0.75 \text{ e}\text{\AA}^{-1}$ (Figure 3 right column). The red part (negative) is localized around the V_6 core, which corresponds to the most nucleophilic regions, while the blue part (positive) is concentrated over the organic ligand and represents the most electrophilic regions. This property reveals the most important features of these hybrid compounds. Figure 4 represents the evolution of the EP minimum, the EP maximum and the difference between these two values. Clearly, a very negative value (V_{10}) implies a better inhibition. Nevertheless, it is difficult to understand the inhibitor behavior inside the functionalized V_6 series from these EP values. The qualitative observation of the EP (Figure 3, right column) indicates that $[\text{V}_6\text{-NO}_2][\text{TBA}]_2$, (compound **2**) and in a less extent the $[\text{V}_6\text{-OH}][\text{TBA}]_2$ (compound **3**, cation TBA) presents additional negative regions. This could help explain why these compounds are good inhibitor candidates.

Ziegler *et al* [56] demonstrated by *ab initio* quantum computation and biochemical investigations, that an increasing positive charge on the vanadyl group increases the inhibition potency of the vanadyl complex on alkaline phosphatase. Different bioactivities for the functionalized V_6 have to be discussed where is the specific binding sites on the enzyme. It is then essential to investigate the possibility of V_6 core to built hydrogen bonds, and the possibilities of functionalized V_6 to have complementary electrostatic potential interactions with the interaction enzyme pocket site. Following the work of Ziegler [56], Mulliken charges belonging to the V-O group have been explored (table 3). We found **2** has the most

nucleophilic oxygen on O1x. We observe that the most charged V-O1x bonds belong to **2**. The specific behavior of **2** is clearer when calculating average Mulliken charges over the three bonds (V-O1x, V-O2x and V-O3x), shown in table 3. Our results are in agreement with those of Ziegler where the more positive V-O bonds allow the complex to bind more tightly to the enzyme [56]. Holtz *et al*, [57] has studied the co-crystallization of alkaline phosphatase complexed with vanadate. They have established the binding site where the vanadate ligand is a modified serine. Previous protein structures show that V₁₀ is bonded *via* hydrogen bond with acid phosphatase [58] and tyrosine kinase [59]. In these two protein structures, V₁₀ anion is linked to enzymes through the amino acids: histidine (His), lysine (Lys), asparagines (Asn), arginine (Arg), moieties which are positively charged or present polar chains.

Therefore, as demonstrated by our *ab initio* calculations and in agreement with the literature, V₆ and V₁₀ core exhibit negative charge, which corresponds to nucleophilic molecular region and in contrary, the organic ligand corresponds to an electrophilic molecular region.

3.2. V₆ binding

In previous studies [34, 35], we have predicted the preferential non-covalent interactions with the different oxygen atoms of the V₁₀ anion in order to explain and predict the behaviour of those species in case of a reaction with protons or cationic groups. A similar analysis has been done on V₆ compounds. The nucleophilic oxygen atoms, which are available on the surface of V₆ as hydrogen bond acceptor, interact with oxygen, nitrogen or carbon atoms of organic moieties as hydrogen donor in order to form hydrogen bonds, such as O_{V6}···HO, O_{V6}···HN, O_{V6}···HC. The carbon atoms of the ligands interact with the oxygen atoms of V₆ through O_{V6}···HC hydrogen bonds. From the structures containing the [V₆O₁₉]²⁻, we have chosen the 18 crystalline structures with six bridged organic ligands (Table 1). In all 18 structures, we have found weak C-H···O bonds due to the fact that V₆ anion is stabilized with large non-polar chain through the network of weak C-H···O bonds. Both O1x and O2x atoms build weak C-H···O bonds. The geometry of C-H···O interactions have been analyzed using the 99 identified non-bonding interactions. Figure 5 and 6 show the results of the CSD search of the C-H···O distances and angles distribution for all intermolecular interactions. In term of angularity, all these interactions follow the trend expected for hydrogen bonds; namely the C-H···O angle opens up as the distance between donor and acceptor increases. C-

H \cdots O interactions are mainly at long distance 2.4 - 2.8 Å and angle from 120-160 ° included in an ellipsoid drawn on Figure 5.

The variation in bond distance and angle for C-H \cdots O interaction (Figure 5 and Figure 6) reflects the different types of interaction: stronger bond, at shorter distances and higher angle binding with oxygen atoms O2x and weaker bond mainly binding with O1x. The percentage of interaction for which $d_{H\cdots O} < 2.5$ Å is 39 % for O2 (respectively 30 % for O1x). It indicates that oxygen atoms O2x is more reactive than oxygen atoms O1x. Therefore, we can confirm that the protonation sites in the cage are oxygen atoms of type O2x. This observation is in agreement with theoretical calculation [60], and our experimental “Atom In Molecules” (AIM) charges, where we have found that O2 atoms are more reactive than O1 [53].

3.3. Localization of protonation basic sites on V₆ core

In order to obtain a quantitative determination of the relative activity and the protonation sites in V₆ anion, we have used the protonated hexavanadate from Table 1 (i.e. PAGSOF, PAGESUL, PAGTAS, KURBOO, KURBUU) and hexavanadate based compounds where more than six oxygen atoms are bridged with organic ligands (Table 2). The hydrogen positions in protonated V₆ are located only in few compounds. The protonation site on all reported V₆ compounds, is at O2x bridging oxygen. Oxygen atoms O1x are not connected with organic ligands. The main protonation site for the protonated V₆ anion is oxygen atom O2x and the main atoms for connection with organic parts is O2x. These results suggest that atom O2x is more reactive than atom O1x. This is in agreement with previous report on theoretical electrostatic potential of a functionalized V₆ (Bu₄N)₂[{FcC(O)NHC(CH₂O)₃]₂V₆O₁₃] [53]. It was found that oxygen charges are O6x (-1.11) < O3x (-0.74) < O2x (-0.68) < O1x (-0.54).

Protonation basic sites of V₆ core have been identified as the doubly bridging oxygen atoms (O2x), establishing these as more nucleophilic/basic than the mono-coordinate oxygen atoms (O1x).

4. Conclusion

Throughout this work, we have studied the reactivity of functionalized hexavanadates V₆. It provides evidence of the oxygen atom type influence on the hydrogen bonding geometry. Analysis of non-covalent interactions between V₆ and organic part using CSD show

that O2x oxygen atoms are more reactive than O1x. We confirm that the protonation sites in the cage are oxygen atoms of type O2x. Increasing concentrations of the synthesized hexavanadates induce the inhibition of Na⁺/K⁺-ATPase activity in a concentration-dependent manner in all cases. IC₅₀ values for each investigated hexavanadate (except 4) were the same order of magnitude (in the range 1 × 10⁻⁵ - 1 × 10⁻⁴ mol/L). The obtained results demonstrate that the most potent inhibitor is compound [V₆-NO₂][TBA]₂ (IC₅₀ = (1.8 ± 0.5) × 10⁻⁵ mol/L). Qualitative observation of the EP indicates that [V₆-NO₂][TBA]₂ and in a less extent [V₆-OH][TBA]₂ presents additional negative regions. We observe from *ab initio* calculations that [V₆-NO₂][TBA]₂ has the most nucleophilic sites on "O2x", and it coincides that it has the most effective inhibitor among **1-5**. This could be the reason why these compounds could be the good inhibitors.

Table of Abbreviations

Abbreviation	Meaning
A	Acceptor
AIM	Atom In Molecules
ARG	Arginine
ATPase	Adenosine TriPhosphatase
CSD	Cambridge Structural Database
DFT	Density Functional theory
EP	Electrostatic Potential
HIS	Histidine
IC₅₀ values	Half maximal inhibitory concentration values
LYS	Lysine
NCI	Non-Covalent Interactions
O1x	Oxygen atom bonded to only one vanadium atom
O2x	Oxygen atom shared between two vanadium atoms
O3x	Oxygen atom connected with two vanadium atoms and organic ligand

O6x	Oxygen atom with a six-fold coordination with vanadium atoms
P_i	Inorganic phosphate group
PMCA	Plasma membrane Ca ²⁺ -ATPase
POMs	Polyoxometalates
POVs	Polyoxovanadates
SEM	standard error of mean
TBA	Tetrabutylammonium
V ₄	Tetranavanadate
V ₆	Hexavanadate
V ₁₀	Decavanadate
V ₁₂	Dodecavanadate

Acknowledgements

XX thanks CSC for scholarship. NBP thanks CentraleSupélec for invited associated professor position. NBP would like to thank the Ministry of Education, Science and Technological Development of the Republic of Serbia for financial support (Project No OI 172043). MBČ, DZK and VMV are grateful to the Ministry of Education, Science and Technological Development of the Republic of Serbia for the financial support (Project No 172023). Theoretical calculations have been made on the computing meso-center of CentraleSupélec.

Highlights

- Functionalized hexavanadates (V₆) inhibit Na⁺/K⁺-ATPase.
- [V₆-OH][Na]₂ inhibited Na⁺/K⁺-ATPase activity up to 30% at max. investigated concentration.
- The O2x bridged oxygen atoms are more reactive than O1x terminal oxygen.
- The protonation sites in the cage are oxygen atoms of type O2x.
- The most charged V-O1x bond belongs to [V₆-NO₂][TBA]₂ TBA (tetrabutylammonium).

References

- [1] M.T. Pope, *Heteropoly and Isopoly Oxometalates*. Berlin: Springer; 1983.
- [2] M.T. Pope, A. Müller, *Polyoxometalate Chemistry: An Old Field with New Dimensions in Several Disciplines*, *Angew. Chem. Int. Ed. Engl.* 30 (1991) 34–48.
- [3] H.K. Chae, G. Walter, V. Klemperer, W. Day, Organometal hydroxide route to $[(C_5Me_5)Rh]_4(V_6O_{19})$, *Inorg. Chem.* 28 (1989) 1423–1424.
- [6] Y. Hayashi, Y. Ozawa, K. Isobe, The First “Vanadate Hexamer” Capped by Four Pentamethylcyclopentadienyl-rhodium or -iridium Groups, *Chem. Lett.* 18 (1989) 425-426.
- [7] Y. Hayashi, Y. Ozawa, K. Isobe, Site-selective oxygen exchange and substitution of organometallic groups in an amphiphilic quadruple-cubane-type cluster. Synthesis and molecular structure of $[(MCp^*)_4V_6O_{19}]$ (M = rhodium, iridium), *Inorg. Chem.* 30 (1991) 1025–1033.
- [8] Q. Chen, D. P. Goshorn, C.P. Scholes, X. L. Tan, J. Zubieta, Coordination compounds of polyoxovanadates with a hexametalate core. Chemical and structural characterization of $[VV_6O_{13}[(OCH_2)_3CR]_2]^{2-}$, $[VV_6O_{11}(OH)_2[(OCH_2)_3CR]_2]$ $[VIV_4VV_2O_9(OH)_4[(OCH_2)_3CR]_2]^{2-}$, and $[VIV_6O_7(OH)_6[(OCH_2)_3CR]_2]^{2-}$, *J. Am. Chem. Soc.* 114 (1992) 4667–468.
- [9] Q. Chen, J. Zubieta, Synthesis and structural characterization of a polyoxovanadate coordination complex with a hexametalate core: $[(n-C_4H_9)_4N]_2[V_6O_{13}\{O_2NC(CH_2O)_3\}_2]$, *Inorg. Chem.* 29 (1990) 1456–1458.
- [10] Q. Chen, J. Zubieta, A novel hexavanadate core: synthesis and structure of the mixed valence cluster $[V_6O_8\{(OCH_2)_3CEt\}_2\{(OCH_2)_2C(CH_2OH)(Et)\}_4]^{2-}$ and a comparison with the hexametalate core of $[V_6O_{13}(OMe)_3\{(OCH_2)_3CCH_2OH\}]^{2-}$, *J. Chem. Soc. Chem. Commun.* (1993) 1180-1182.
- [11] J. W. Han, K.I. Hardcastle, C. L. Hill, Redox-Active Coordination Polymers from Esterified Hexavanadate Units and Divalent Metal Cations, *Eur. J. Inorg. Chem.* 13 (2006) 2598–2603.
- [12] J.W. Han, C.L. Hill, A coordination network that catalyzes O_2 based oxidations, *J. Am. Chem. Soc.* 129 (2007) 15094-15095.

- [13] Y. Hayashi, Hetero and Lacunary Polyoxovanadate Chemistry: Synthesis, Reactivity and Structural Aspects, *Coord. Chem. Rev.* 255 (2011) 2270-2280.
- [14] L. Ma, S. Liu, J. Zubieta, Synthesis and characterization of a trinuclear polyoxomolybdate containing a reactive $[\text{MoO}_3]$ unit, $[(n\text{-C}_4\text{H}_9)_4\text{N}]_2[\text{Mo}_3\text{O}_7(\text{CH}_3\text{C}(\text{CH}_2\text{O})_3)_2]$, and its conversion to the methoxy derivative $[(n\text{-C}_4\text{H}_9)_4\text{N}][\text{Mo}_3\text{O}_6(\text{OCH}_3)(\text{CH}_3\text{C}(\text{CH}_2\text{O})_3)_2]$, *Inorg. Chem.* 28 (1989) 175–177.
- [15] P. Yin, Wu Pingfan, X. Zicheng, D. Li, E. Bitterlich, J. Zhang, P. Cheng, D.V. Vezenov, T. Liu, Y. Wei, A Double-Tailed Fluorescent Surfactant with a Hexavanadate Cluster as the Head Group, *Angew. Chem. Int. Ed.* 50 (2011) 2521–2525.
- [16] P. Wu, Z. Xiao, J. Zhang, J. Hao, J. Chen, P. Yin, Y. Wei, Y. DMAP-catalyzed esterification of pentaerythritol-derivatized POMs: a new route for the functionalization of polyoxometalates, *Chem. Commun.* 47 (2011) 5557-5559.
- [17] C. Daniel, H. Hartl, Neutral and Cationic $\text{V}^{\text{IV}}/\text{V}^{\text{V}}$ Mixed-Valence Alkoxopolyoxovanadium Clusters $[\text{V}_6\text{O}_7(\text{OR})_{12}]^{n+}$ ($\text{R} = -\text{CH}_3, -\text{C}_2\text{H}_5$): Structural, Cyclovoltammetric and IR-Spectroscopic Investigations on Mixed Valency in a Hexanuclear Core, *J. Am. Chem. Soc.* 127 (2005) 13978-13987.
- [18] D. Krstić, M. Colović, N. Bošnjaković-Pavlović, A. Spasojević-de Biré, V. Vasić, Influence of decavanadate on rat synaptic plasma membrane ATPases activity, *Gen. Physiol. Biophys.* 28 (2009) 302–308
- [19] D.L. Stokes, F. Delavoie, W.J. Rice, P. Champeil, D.B. McIntosh, J.J. Lacapère, Structural studies of a stabilized phosphoenzyme intermediate of Ca^{2+} -ATPase, *J. Biol. Chem.* 280 (2005) 18063–18072.
- [20] L.A. Vasilets, W. Schwarz, Structure-function relationships of cation binding in the Na^+/K^+ -ATPase, *Biochim. Biophys. Acta.* 1154 (1993) 201–222
- [21] G. Rodriguez de Lores Arnaiz, C. Peña, Characterization of synaptosomal membrane Na^+/K^+ ATPase inhibitors, *Neurochem. Int.* 27 (1995) 319–327.
- [22] a) D. Krstić, K. Krinulović, G. Joksić, V. Spasojević – Tisma, T. Momić, V. Vasić, Effects of digoxin and gitoxin on the enzymatic activity and kinetic parameters of Na^+/K^+ -ATPase, *J. Enz. Inhib. Med. Chem.* 19 (2004) 409–415. b) D. Krstić; K. Krinulović; V. Vasić, Inhibition of Na^+/K^+ -ATPase and Mg^2+ -ATPase by metal ions and prevention and recovery of inhibited activity by chelators, *J. Enz. Inhib. Med. Chem.* 20 (2005) 469–476. c) J. Z. Blasiak, Cooperative binding of the organophosphate paraoxon to the Na^+/K^+ -ATPase, *Naturforsch.* 50c (1995) 660–663.

- [23] I. Matsuoka, S.J. Ohkubo, ATP- and adenosine-mediated signaling in the central nervous system: adenosine receptor activation by ATP through rapid and localized generation of adenosine by ecto-nucleotidases, *Pharmacol. Sci.* 94 (2004) 95–99.
- [24] G. Scheiner-Bobis, The sodium pump. Its molecular properties and mechanics of ion transport, *Eur. J. Biochem.* 269 (2002) 2424–33.
- [25] F. Lefranc, T. Mijatović, Y. Kondo, S. Sauvage, I. Roland, D. Krstić, V. Vasić, P. Gailly, S. Kondo, G. Blanco, R. Kiss, Targeting the alpha 1 subunit of the sodium pump to combat glioblastoma cells, *Neurosurgery* 62 (2008) 211–21.
- [26] M. Aureliano, Vanadate oligomer inhibition of passive and active Ca^{2+} translocation by the Ca^{2+} pump of sarcoplasmic reticulum, *J. Inorg. Biochem.* 80 (2000) 145–147.
- [27] D.W. Boyd, K. Kustin, M. Niwa, Do vanadate polyanions inhibit phosphotransferase enzymes?, *Biochim. Biophys. Acta.* 827 (1985) 472–47.
- [28] a) R.J. Pezza, M.A. Villarreal, G.G. Montich, C.E. Argarana, Vanadate inhibits the ATPase activity and DNA binding capability of bacterial MutS. A structural model for the vanadate-MutS interaction at the Walker A motif, *Nucleic Acids Res.* 3 (2002) 4700–4708. b) J.M. Messmore, R.T. Raines, Decavanadate inhibits catalysis by ribonuclease A, *Arch. Biochem. Biophys.* 381 (2000) 25–30.
- [29] a) D.C. Crans, M. Mahroof-Tahir, O.P. Anderson, M.M. Miller, X-ray structure of $(\text{NH}_4)_6(\text{Gly-Gly})\text{V}_{10}\text{O}_{28} \times 4\text{H}_2\text{O}$. Model studies for polyoxometalates - protein interactions, *Inorg. Chem.* 33 (1994) 5586-5590. b) K. Stroobants, D. Saadallah, G. Bruylants, T.N. Parac-Vogt, Thermodynamic study of the interaction between hen egg white lysozyme and Ce(IV)-Keggin polyoxotungstate as artificial protease, *Phys. Chem. Chem. Phys.* 16 (2014) 21778-21787.
- [30] M. Aureliano, R.M.C. Gândara, Decavanadate effects in biological systems, *J. Inorg. Biochem.* 99 (2005) 979–985.
- [31] D.L. Stokes, F. Delavoie, W.J. Rice, P. Champeil, D.B. McIntosh, J.J. Lacapère, Structural Studies of a Stabilized Phosphoenzyme Intermediate of Ca^{2+} -ATPase, *J. Biol. Chem.* 280 (2005) 18063–18072.
- [32] T. Tiago, M. Aureliano, C. Gutiérrez–Merino, Decavanadate binding to a high affinity site near the myosin catalytic centre inhibits F-actin-stimulated myosin ATPase activity, *Biochemistry.* 43 (2004) 555c1–5561.
- [33] a) M. Aureliano, Decavanadate contribution to vanadium biochemistry: In vitro and in vivo studies. *Inorg. Chimica Acta* 420 (2014) 4-7 b) M. Aureliano, C. André Ohlin

- Decavanadate in vitro and in vivo effects: facts and opinions, *J. Inorg. Biochem.* 137 (2014) 123–130.
- [34] N. Bošnjaković-Pavlović, A. Spasojević-de Biré, I. Tomaz, N. Bouhaida, F. Avecilla, U. Mioc, J. Costa Pessoa, N. E. Ghermani, Electron and electrostatic properties of a cytosine decavanadate compound from high resolution x-ray diffraction: toward a better understanding of chemical and biological properties of decavanadates, *Inorg. Chem.* 48 (2009) 9742-9753.
- [35] N. Bošnjaković-Pavlović, J. Prévost, A. Spasojević – de Biré, Crystallographic statistical study of decavanadate anion based structure: toward the prediction of noncovalent interactions, *Cryst. Growth & Des.* 11 (2011) 3778–3789.
- [36] F. Ping-Ping, W. Xin-Long, W. En-Bo, Q. Chao, X. Lin. Synthesis, Structure Characterization and Biological Activity of a Novel Polyoxovanadate Cluster: $[\text{NH}_3(\text{CH}_2)_2\text{NH}_2(\text{CH}_2)_2\text{NH}_3]_4\cdot[\text{V}^{\text{V}}_6\text{V}^{\text{IV}}_{12}\text{O}_{42}(\text{PO}_4)](\text{PO}_4)\cdot 2\text{H}_2\text{O}$, *Chem. Res. Chinese.* 21(4)(2005) 381-385.
- [37] T. Yamase, Medical chemistry of polyoxometalates. Part 1. Potent antitumor activity of polyoxomolybdates on animal transplantable tumors and human cancer xenograft, *Inorg Chim Acta* 15 (1988) 15–8.
- [38] T. Yamase, Polyoxometalates for molecular devices: antitumor activity and luminescence, *Mol. Eng.* 3 (1993) 241–62.
- [39] H. Yanagie, A. Ogata, S. Mitsui, T. Hisa, T. Yamase, M. Eriguchi, Anticancer activity of polyoxomolybdate, *Biomed. Pharmacother.* 60 (2006) 349–352.
- [40] F.H. Allen, The Cambridge Structural Database: a quarter of a million crystal structures and rising, *Acta Cryst.* B58 (2002) 380–388.
- [41] (a) T. Steiner, The hydrogen bond in the solid state, *Angew. Chem. Int. Ed.* 41 (2002) 49–76. (b) R. Taylor, O. Kennard, Crystallographic evidence for the existence of C-H...O, C-H...N, and C-H...Cl hydrogen bonds, *J. Am. Chem. Soc.* 104 (1982) 5063–5070.
- [42] a) G.R. Desiraju, The C–H...O Hydrogen Bond: Structural Implications and Supramolecular Design, *Acc. Chem. Res.* 29 (1996) 441–449. b) G.R. Desiraju, T. Steiner, The weak hydrogen bond in structural chemistry and biology, Oxford University Press, 1999
- [43] G. Bogdanović, A. Spasojević-de Biré, S. Zarić, Evidence of a C-H... π interaction between an organic moiety and a chelate ring in transition metal complexes based on crystal structures and computations, *Eur. J. Inorg. Chem.* 7 (2002) 1599-1602.

- [44] H.M. Berman, M.J. Gabanyi, R. Colin, Groom, J.E. Johnson, G.N. Murshudov, R.A. Nicholls, V. Reddy, T. Schwede, M.D. Zimmerman, J. Westbrook, W. Minor, Data to knowledge: how to get meaning from your result, *IUCrJ* 2 (2015) 45–58.
- [45] P.Wu, J.Chen, P.Yin, Z.Xiao, J.Zhang, A.Bayaguud, Y.Wei, Solvent induced supramolecular chiralityswitching of bis (trisalkoxy) hexavanadate, *Polyhedron* 52 (2013) 1344–1348.
- [46] P. Wu, Z. Xiao, J. Zhang, J. Hao, J. Chen, P. Yin, Y. Wei, DMAP catalyzed esterification of pentaerythritol derivatized POMs: a new route for the functionalization of polyoxometalates, *Chem.Commun.* 47 (2011) 5557–5559.
- [47] V. Vasić, D. Jovanović, D. Krstić, G. Nikezić, A. Horvat, L. Vujisić, N. Nedeljković, Prevention and recovery of CuSO₄ induced inhibition of Na,K-ATPase and Mg-ATPase in rat brain synaptosomes by EDTA, *Toxicol. Lett.* 110 (1999) 95-104.
- [48] (a) M.P. Santoni, A.K. Pal, G.S. Hanan, M.C. Tang, K. Venne, A. Furtos, P. Ménard Tremblay, C. Malveau, B. Hasenknopf, Coordination-driven self-assembly of polyoxometalates into discrete supramolecular triangles, *Chem. Commun.* 48 (2012) 200-202. (b) M.P. Santoni, A.K. Pal, G.S. Hanan, A. Proust, B. Hasenknopf, Discrete covalent organic-inorganic hybrids: terpyridine functionalized polyoxometalates obtained by a modular strategy and their metal complexation, *Inorg Chem.* 50 (14) (2011) 6737-45. (c) P. Wu, Z. Xiao, J. Zhang, J. Hao, J. Chen, P. Yin, Y. Wei, DMAP-catalyzed esterification of pentaerythritol-derivatized POMs: a new route for the functionalization of polyoxometalates, *Chem. Commun.* 47 (2011) 5557-5559. (d) D. Li, J. Song, P. Yin, S. Simotwo, A.J. Bassler, Y.Y. Aung, J.E. Roberts, K.I. Hardcastle, C.L. Hill, Tianbo Liu, Inorganic–Organic Hybrid Vesicles with Counterion- and pH-Controlled Fluorescent Properties, *J.Am.Chem.Soc.* 133 (2011) 14010–14016. (e) C. A. S. Favette, L.M. Chamoreau, J. Vaissermann, L. Ruhlmann, B. Hasenknopf, Hybrid Organic–Inorganic Porphyrin–Polyoxometalate Complexes, *Eur. J. Inorg. Chem.* 2008(22) (2008) 3433-3441. (f) Q. Chen, J.A. Zubieta, Structural investigation of the hexavanadate core in oxidized, mixed valence and reduced clusters of the type $[V_{6-n}^V V_n^{IV} O_{13-n}(OH)_S \{(OCH_2)_3CR\}_2]^2$ n=0.3.6, *Inorg Chim Acta* 95 (1992) 198-200.
- [49] (a) E. Scales, L. Sorace, A. Dei, A. Caneschi, C.A. Muryn, D. Collison, E.J.L. McInnes, *Chemical Science* 1 (2010) 221-225. (b) C. Daniel, H. Hartl, A mixed-valence V(IV)/V(V) alkoxo-polyoxovanadium cluster series $[V_6O_8(OCH_3)_{11}]^{n+/-}$: exploring the influence of a mu-oxo ligand in a spin frustrated structure, *Inorg Chim Acta* 131 (2009) 5101-5114. (c) C.

- Aronica, G. Chastanet, E. Zueva, S.A. Borshch, J. M. Clemente-Juan, D. Luneau, A polyoxoalkoxovanadium (III, IV) with a calixarene macrocycle crown. A first example of mixed-valence vanadium (III, IV), *J. Am. Chem. Soc.* 130 (2008) 2365-2371. (d) M.A. Augustyniak-Jabłokow, S. Borshch, C. Daniel, H. Hartl, Y.V. Yablokov, EPR study of the magnetic states of a mixed-valence $V^{IV}_4 V^V_2$ alkoxypolyoxovanadium cluster, *New J. Chem.* 29 (2005) 1064-1071. (e) C. Daniel, H. Hartl, Neutral and cationic V(IV)/V(V) mixed-valence alkoxo-polyoxovanadium clusters $[V_6O_7(OR)_{12}]^{n+}$ (R = -CH₃, -C₂H₅): structural, cyclovoltammetric and IR-spectroscopic investigations on mixed valency in a hexanuclear core, *J. Am. Chem. Soc.* 127 (2005) 13978-87. (f) J. Spandl, C. Daniel, I. Brüdgam, H. Hartl, Synthesis and Structural Characterization of Redox-Active Dodecamethoxoheptaaxohexavanadium Clusters, *Angew. Chem. Int. Ed. Engl.* 42 (2003) 1163–1166.
- [50] M.J. Frisch, G.W. Trucks, H.B. Schlegel, G.E. Scuseria, M.A. Robb, J.R. Cheeseman, G. Scalmani, V. Barone, B. Mennucci, G.A. Petersson, H. Nakatsuji, M. Caricato, X. Li, H.P. Hratchian, A.F. Izmaylov, J. Bloino, G. Zheng, J.L. Sonnenberg, M. Hada, M. Ehara, K. Toyota, R. Fukuda, J. Hasegawa, M. Ishida, T. Nakajima, Y. Honda, O. Kitao, H. Nakai, T. Vreven, J.A. Montgomery, J.E. Peralta, F. Ogliaro, M. Bearpark, J.J. Heyd, E. Brothers, K.N. Kudin, V.N. Staroverov, T. Keith, R. Kobayashi, J. Normand, K. Raghavachari, A. Rendell, J.C. Burant, S.S. Iyengar, J. Tomasi, M. Cossi, N. Rega, J.M. Millam, M. Klene, J.E. Knox, J.B. Cross, V Bakken, C. Adamo, J. Jaramillo, R. Gomperts, R.E. Stratmann, O. Yazyev, A.J. Austin, R. Cammi, C. Pomelli, W.J. Ochterski, R.L. Martin, K. Morokuma, V.G. Zakrzewski, G.A. Voth, P. Salvador, J.J. Dannenberg, S. Dapprich, A.D. Daniels, O. Farkas, J.B. Foresman, J.V. Ortiz, J. Cioslowski, D.J. Fox Gaussian, Inc., Wallingford CT, 2010.
- [51] a) A.D.J. Becke, Density functional thermochemistry. III. The role of exact exchange, *Chem. Phys.* 98 (1993) 5648-5652 b) Y. Zhao, D.G. Truhlar, The M0₆ suite of density functionals for main group thermochemistry, thermochemical kinetics, noncovalent interactions, excited states, and transition elements: two new functionals and systematic testing of four MO₆-class functionals and 12 other functionals, *Theor. Chem. Acc.* 120 (2008) 215–41 c) J.P. Perdew, Density-functional approximation for the correlation energy of the inhomogeneous electron gas, *Phys. Rev.* B33 (1986) 8822–8824.
- [52] a) V.A. Rassolov, M.A. Ratner, J.A. Pople, P.C. Redfern, L.A. Curtiss, 6-31G* basis set for third-row atoms, *J. Comp. Chem.* 22 (2001) 976–984 b) R.C. Binning, L.A. Curtiss,

- Compact contracted basis sets for third-row atoms: Ga–Kr, *J. Comp. Chem.* 11 (1990) 1206-1216.c) T.H.Jr. Dunning, Gaussian Basis Sets for Use in Correlated Molecular Calculations. I. The Atoms Boron Through Neon and Hydrogen, *J. Chem. Phys.* 90 (1989) 1007-1023.
- [53] X. Xu, “Experimental and theoretical charge density analysis of functionalized polyoxovanadates: toward a better understanding of chemical bonding and chemical reactivity”, 2015, PhD thesis. Ecole Centrale Paris, 2015. English
- [54] M.I. Khan, Q. Chen, J. Zubieta, D.P. Goshorn, Hexavanadium polyoxoalkoxide anion clusters: structures of the mixed-valence species $(\text{Me}_3\text{NH})[\text{VIV}_5\text{VVO}_7(\text{OH})_3\{\text{CH}_3\text{C}(\text{CH}_2\text{O})_3\}_3]$ and of the reduced complex $\text{Na}_2[\text{VIV}_6\text{O}_7\{\text{CH}_3\text{CH}_2\text{C}(\text{CH}_2\text{O})_3\}_4]$, *Inorg. Chem.* 31(9) (1992)1556-1558.
- [55] A. Müller, J. Meyer, H. Bogge, A. Stammli, A.Y. Botar, Cis-/Trans-Isomerie bei Bis-(trisalkoxy)-hexavanadaten - Cis- $\text{Na}_2[\text{V-6(IV)O-7(OH)}_6((\text{OCH}_2)_3\text{CCH}_2\text{OH})_2] \cdot 8\text{H}_2\text{O}$, cis- $(\text{CN}_3\text{H}_6)_3[\text{V-5(IV)O-V}_{13}((\text{OCH}_2)_3\text{CCH}_2\text{OH})_2] \cdot 4,5\text{H}_2\text{O}$ und trans- $(\text{CN}_3\text{H}_6)_2[\text{V-6(V)O-13}((\text{OCH}_2)_3\text{CCH}_2\text{OH})_2] \cdot \text{H}_2\text{O}$, *Anorg. Allg. Chem.* 621 (1995) 1818–1831.
- [56] A.J. Ziegler, J. Florian, M.A. Ballicora, A.W. Herlinger, Alkaline phosphatase inhibition by vanadilbdketone complexes:electron density effects, *J. Enzyme Inhib. Med. Chem.* 24 (2009) 22-28.
- [57] M.H. Kathleen M, B. Stec, E. R. Kantrowitz, A Model of the Transition State in the Alkaline Phosphatase Reaction, *J. Biol. Chem.* 274 (1999) 8351-8354.
- [58] L.R. Felts, J.T. Reilly, J.J. Tanner Structure of Francisella tularensis AcpA: prototype of a unique superfamily of acid phosphatases and phospholipases *J. Biol. Chem.* 281 (2006) 30289-30298.
- [59] J.H. Bae, E.D. Lew, S. Yuzawa, F. Tome, I. Lax, J. Schlessinger, The selectivity of receptor tyrosine kinase signaling is controlled by a secondary SH2 domain binding site.*Cell (Cambridge, Mass.)* 138 (2009) 514-524.
- [60] J. Schulz, R. Gyepes, I. Císařová, P. Štěpnička, Synthesis, structural characterisation and bonding in an anionic hexavanadate bearing redox-active ferrocenyl groups at the periphery, *New J. Chem.* 34 (2010) 2749-2756.

List of Figures

Figure 1 Labeling scheme and type of atoms in the functionalized V6 ion. (a) Structure of functionalized V6 anion; (b) Atomic surroundings of V atom.

Figure 2. The influence of various concentrations of hexavanadates **1-5** on the activity of commercially available, purified porcine cerebral cortex Na^+/K^+ -ATPase. The residual enzyme activity is expressed as a percent of the control value (the enzyme activity obtained in the absence of the inhibitor). The values are expressed as mean \pm S.E.M. The plots of experimental values are fitted by sigmoidal functions.

Figure 3. Theoretical electrostatic potential (EP) ($\text{e}\cdot\text{\AA}^{-1}$) mapped on isodensity surface ($0.007 \text{ e}\cdot\text{\AA}^{-3}$) (second column) and isosurface of theoretical electrostatic potential (EP) ($\text{e}\cdot\text{\AA}^{-1}$) for $[\text{V}_6\text{CH}_3]$, $[\text{V}_6\text{NO}_2]$, $[\text{V}_6\text{OH}]$ and $[\text{V}_6\text{-C}_3]$. First column: molecular structure.

Figure 4. Theoretical EP values ($\text{e}\cdot\text{\AA}^{-1}$) at the molecular surface for V_{10} and for the functionalized V_6 series.

Figure 5. Distribution of distances and angles for CH...O interactions according to the different oxygen types in the CSD V_6 series from table 1.

Figure 6. a) Distribution of the C-H...O distances b) Distribution of the value of the C-H..O angles in the CSD V_6 series from table 1.

List of Tables

Table 1. List of arm-like functionalized V_6 used in this paper. The number of non-covalent interactions (NCI) is given in the last column. In Parentheses the NCI number concerning the $\text{O}1\text{x}$ (respectively $\text{O}2\text{x}$ in bold).

Table 2. List of V_6 bridged with more than six organic ligands.

Table 3 Inhibition parameters (IC_{50} values (10 min) for V_6 of commercially purified Na^+/K^+ -ATPase. The size of the anion, modeled by the longest distance between opposite atoms of the organic part is given. V_{10} : decavanadate $[\text{V}_{10}\text{O}_{28}]^{6-}$.

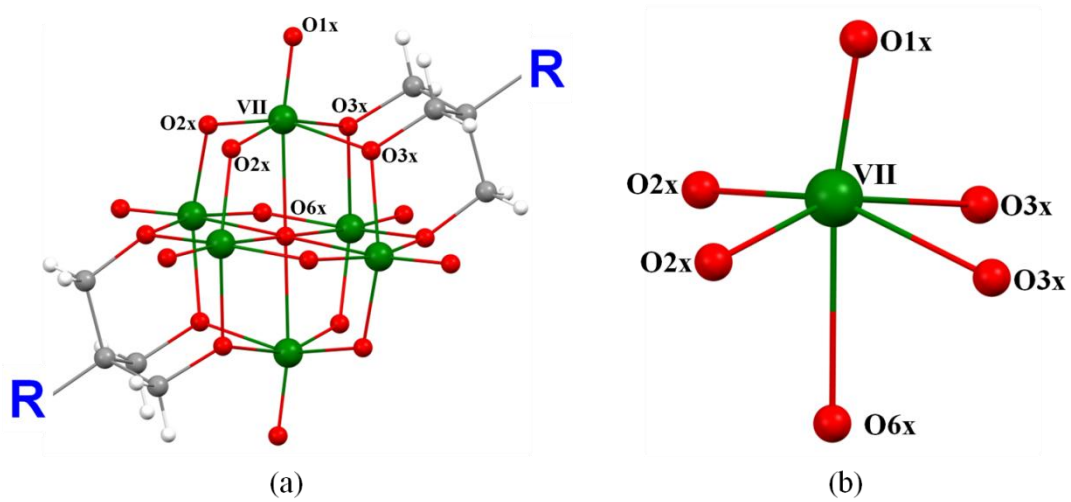


Figure 1

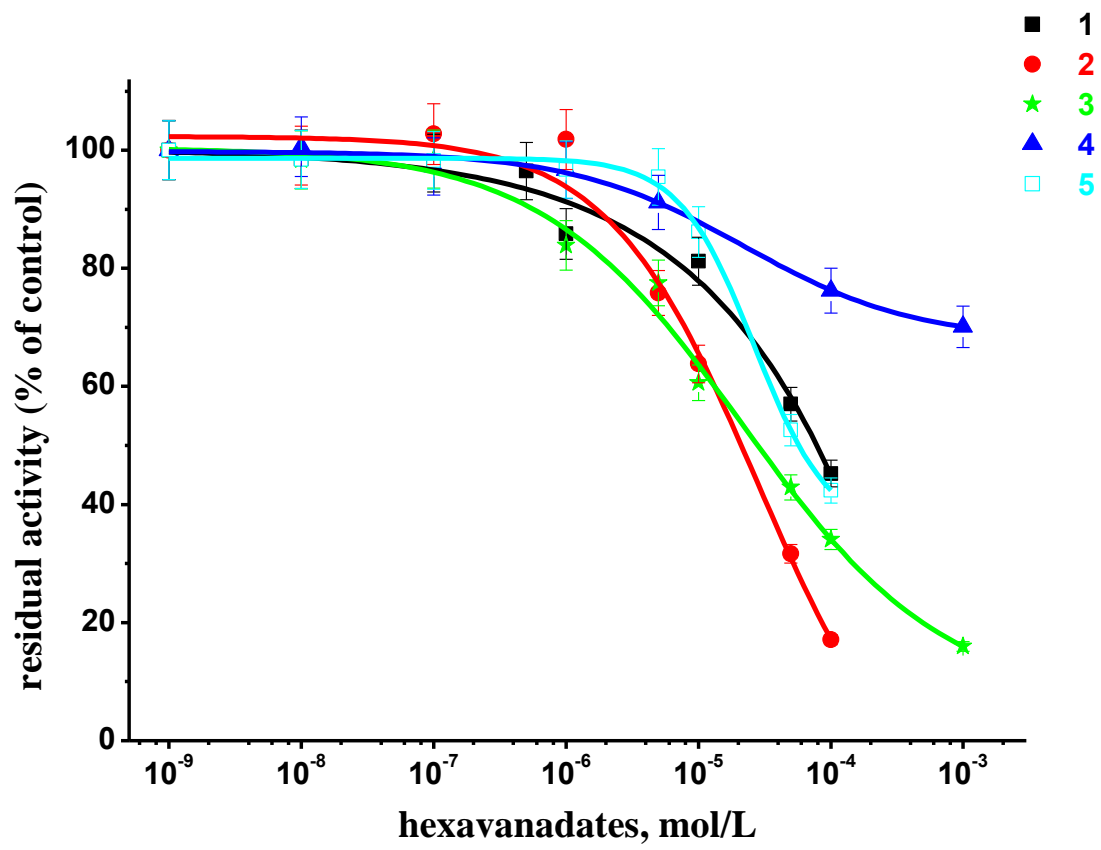


Figure 2.

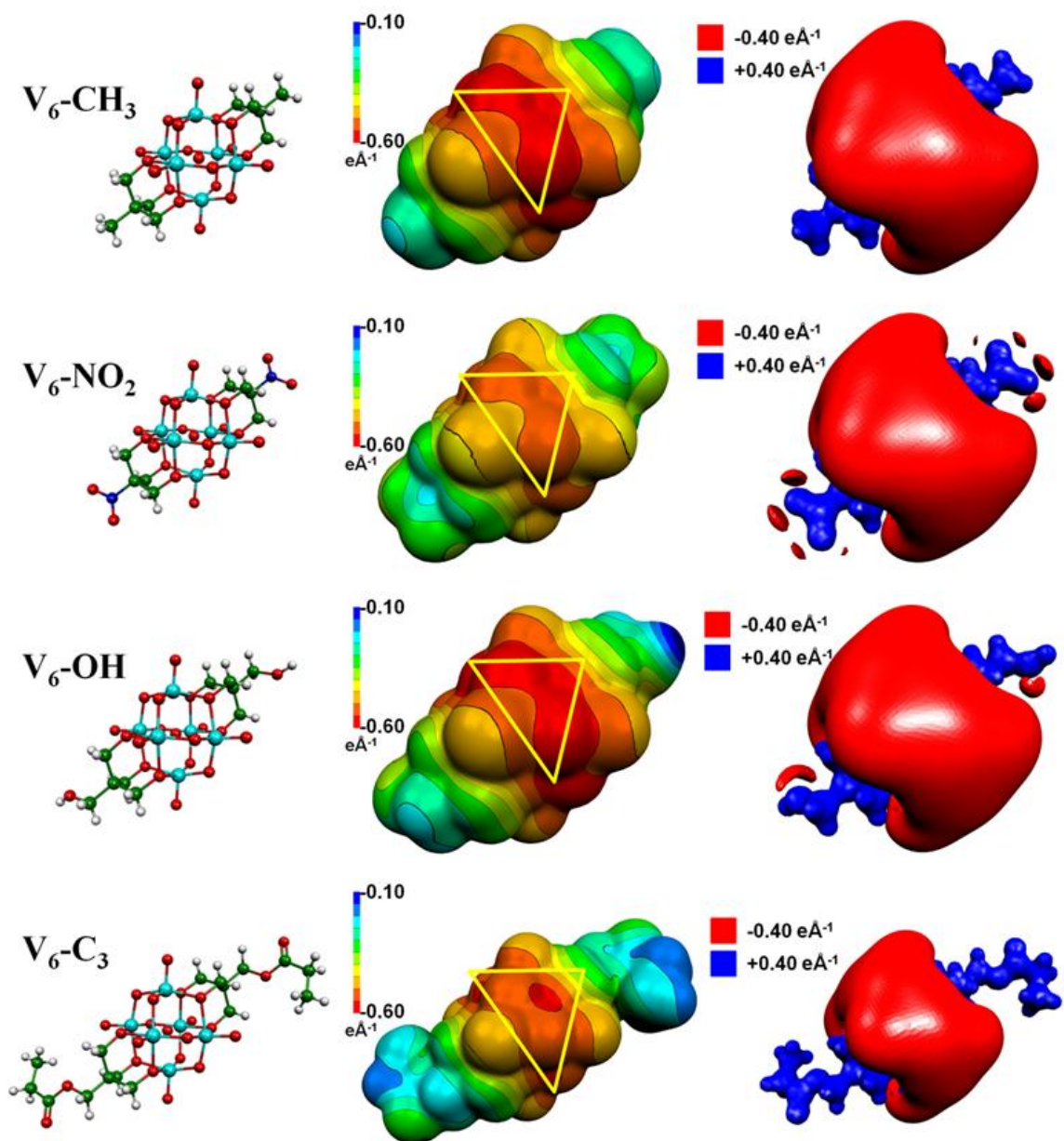


Figure 3.

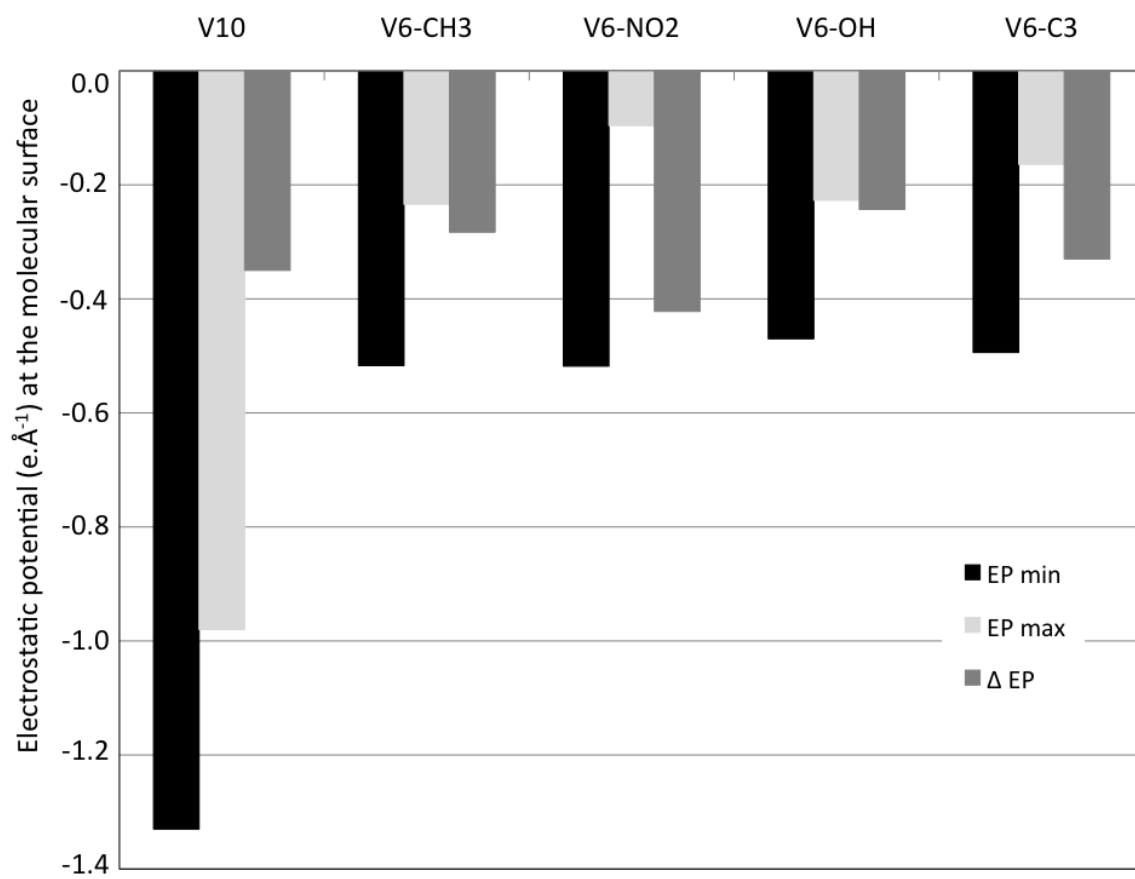


Figure 4.

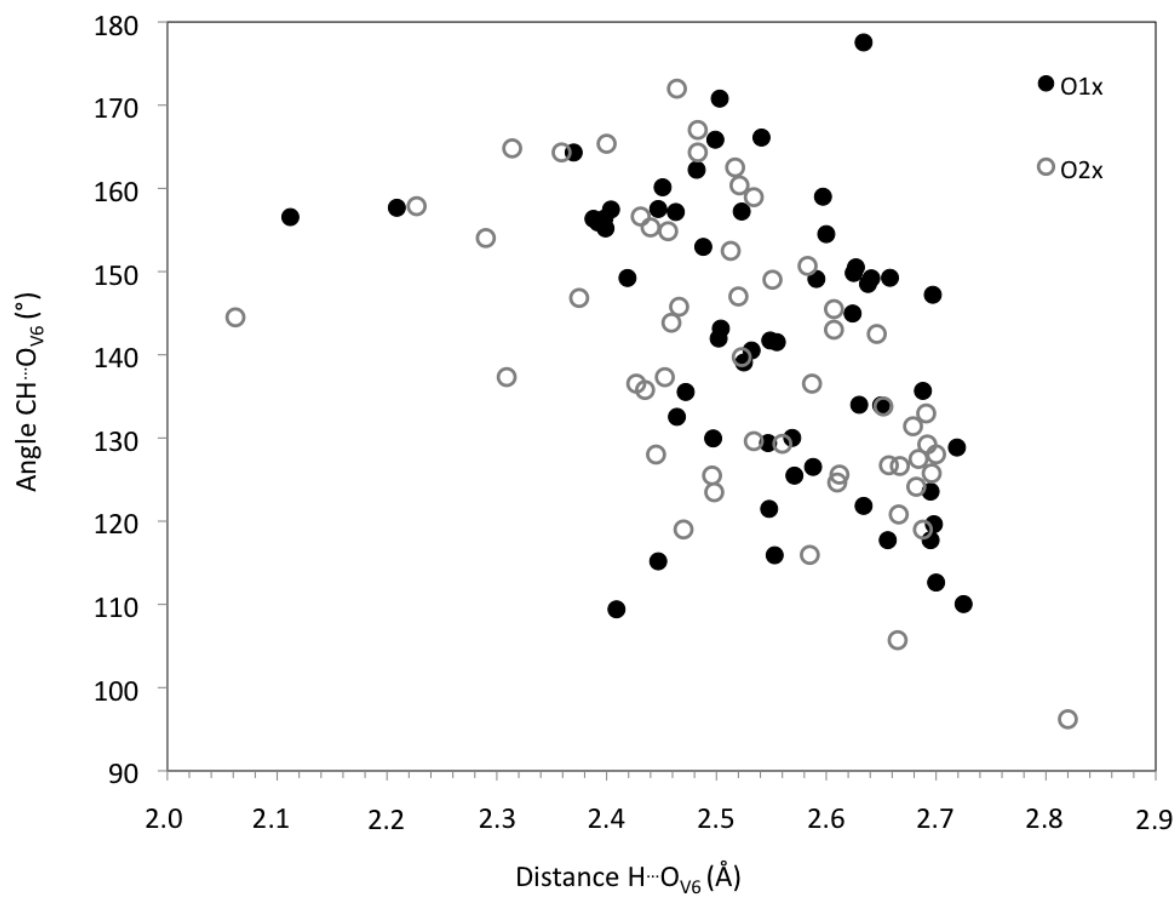


Figure 5.

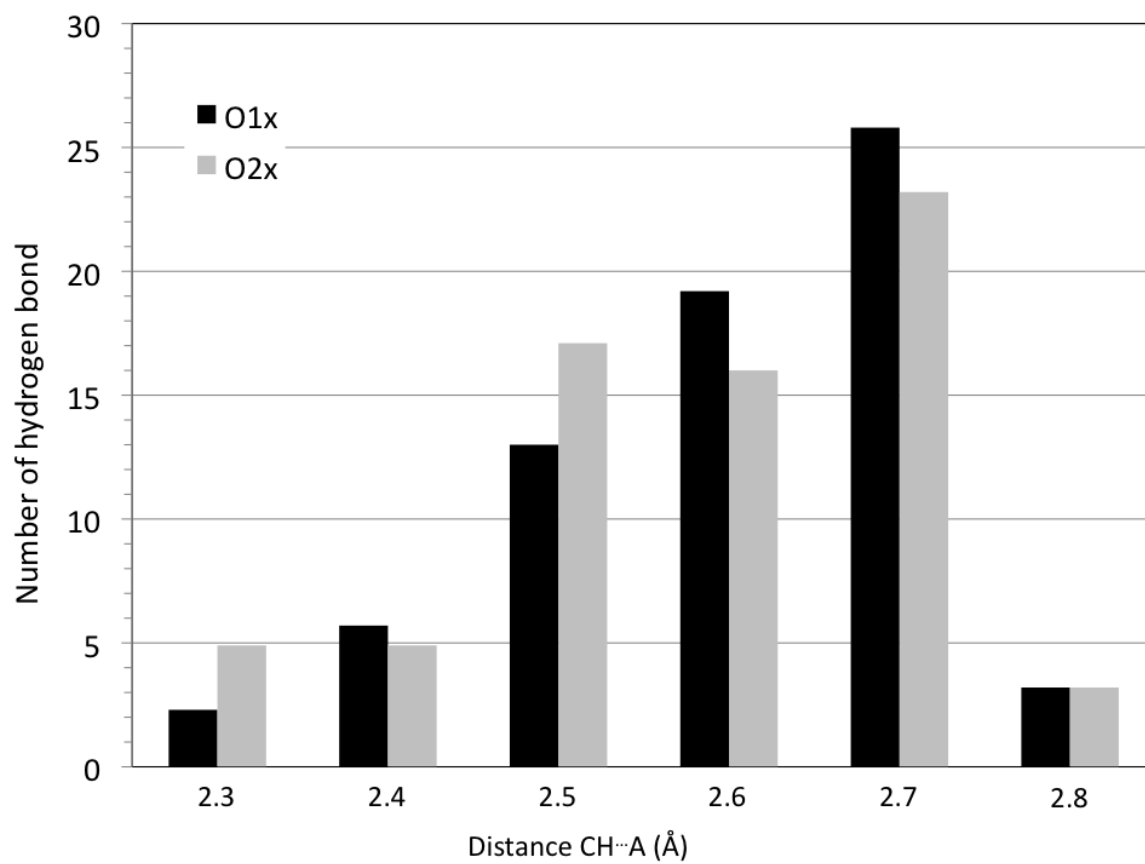


Figure 6. a

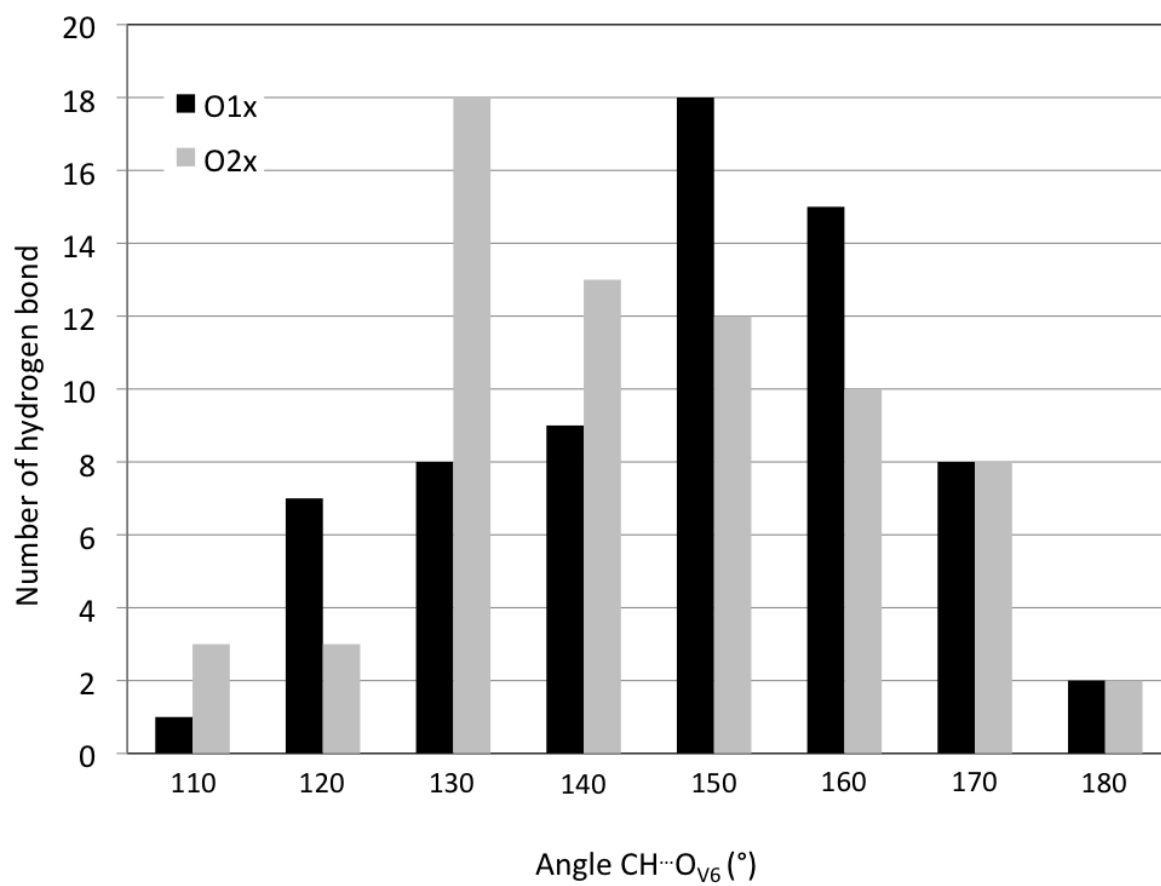
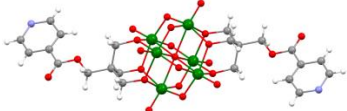
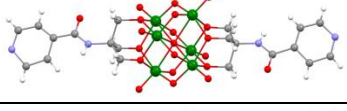
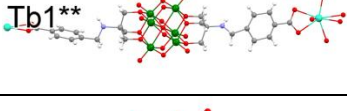
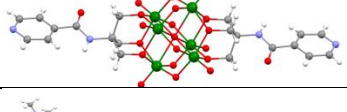
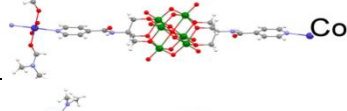
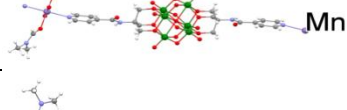
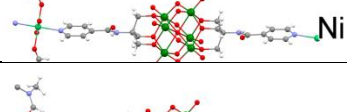
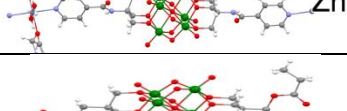
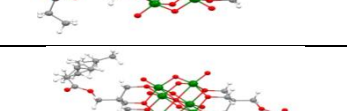
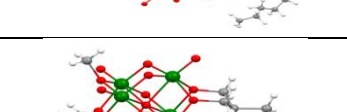
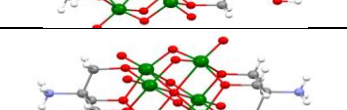
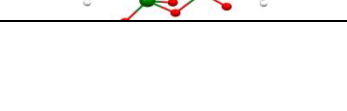


Figure 6. b

Table 1.

Refcode	Structure of functionalized Hexavanadate	R factor	Cation or other segment	Reference	Total number of NCI (O1x/O2x)
Non-protonated V ₆					
EGEMUZ		7.7	TBA ⁺	48e	10(6/4)
EGENEK		8.75	TBA ⁺ , CH ₃ CN,	48e	7(2/5)
LOFVUY		8.79	Tb ²⁺ , (CH ₃) ₂ NCHO	12	6(3/3)
NEMDEP		6.74	TBA ⁺ , N(CH ₃) ₂ CHO	11	7(1/6)
NEMDIT		7.78	Co ²⁺ , N(CH ₃) ₂ CHO	11	8(7/1)
NEMDOZ		9.76	Mn ²⁺ , N(CH ₃) ₂ CHO	11	5(4/1)
NEMDUF		9.73	Ni ²⁺ , N(CH ₃) ₂ CHO	11	5(4/1)
NEMFAN		8.98	Zn ²⁺ , N(CH ₃) ₂ CHO	11	9(5/4)
OQETOU		5.76	TBA ⁺	48c	6(3/3)
OQETUA		4.13	TBA ⁺	48c	6(1/5)
PELYIO		6.62	TBA ⁺	14	8(1/7)
SAJWEH		7.81	CH ₃ SOCH ₃	48d	3(2/1)

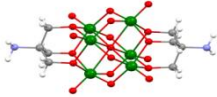
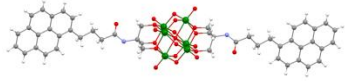
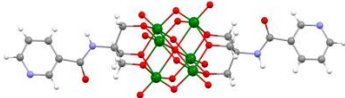
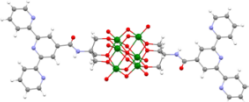
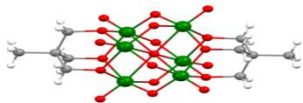
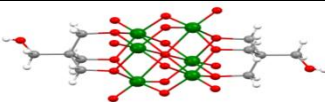
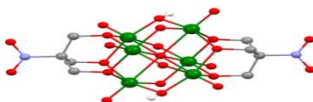
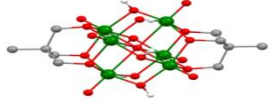
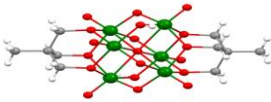
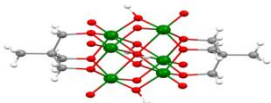
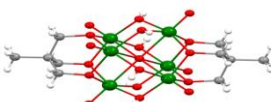
SAJWIL		4.18	TBA ⁺	48d	6(3/3)
SAJWOR		8.67	TBA ⁺ , N(CH ₃) ₂ CHO,	48d	2(2/0)
SAMMOK		4.13	TBA ⁺ , N(CH ₃) ₂ CHO	48a	4(2/2)
UCOTEN		5.29	TBA ⁺ , N(CH ₃) ₂ CHO	48b	4(2/2)
VERDEB10		5.5	TBA ⁺	8	5(3/2)
VERDIF10		4.9	TBA ⁺ , N(CH ₃) ₂ CHO	9	4(1/3)
Protonated V₆					
Refcode	Structure of functionalized	R facto	Cation or other segment	Reference	Bridged O atom
KURBOO		5.8	TBA ⁺ , CH ₂ Cl ₂	48f	O2
KURBUU		5.8	TBA ⁺ , C ₁₂ H ₁₂ N ₂	48f	O2
PAGSOF		4.3	(C ₂ H ₅) ₂ O, N(CH ₃) ₂ CHO	8	O2
PAGSUL		4.3	TBA ⁺	8	O2
PAGTAS		4.2	TBA ⁺ , CH ₂ Cl ₂ , C ₁₂ H ₁₂ N ₂	8	O2

Table 2.

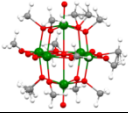
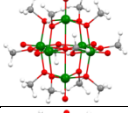
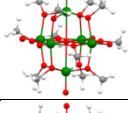
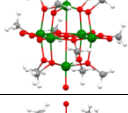
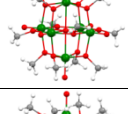
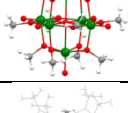
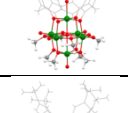
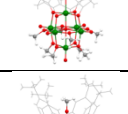
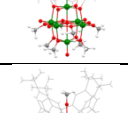
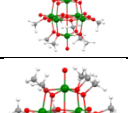
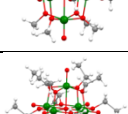
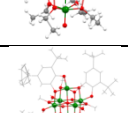
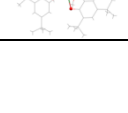
Refcode	Structure of functionalized Hexavanadate	R factor	Cation or other segment	Reference
FUSLEL		3.18	-	48e
MUXTAA		4.24	-	48e
MUXTAA01		2.82	-	12
MUXTAA02		2.82	-	11
MUXTEE		7.36	TBA ⁺ , CH ₃ OH	11
MUXTOO		4.37	TBA ⁺	11
NOBDAK		5.18	Et ₄ N ⁺	11
NOBDEO		7.38	NH ₄ ⁺	11
NOBDIS		5.04	(C ₂ H ₅) ₃ NH ⁺	48c
NOBDOY		5.75	C ₅ H ₆ N ⁺	48c
QAWDUO		3.59	SbCl ₆ ⁻	14
XADMEU01		4.94	-	48d
MUVLUL		7.24	CH ₃ OH, H ₂ O	48d

Table 3

Number	Compound	Structure	IC ₅₀ , (mol/L)	Length (Å)	Average oxygen (O1x, O2x) Mulliken charges
1	[V ₆ -CH ₃][TBA] ₂		7.6×10^{-5}	11.27	0.5925
2	[V ₆ -NO ₂][TBA] ₂		1.8×10^{-5}	12.48	0.602
3	[V ₆ -OH][TBA] ₂		2.9×10^{-5}	12.93	0.5922
4	[V ₆ -OH][Na] ₂		$> 10^{-3}$	12.93	
5	[V ₆ -C ₃][TBA] ₂		5.5×10^{-5}	16.49	0.5925
V ₁₀	[V ₁₀ O ₂₈] ⁶⁻		1.71×10^{-6}	9.40	